Canadian Journal of Forest Research

OPEN ACCESS | Article

Mapping large European aspen (*Populus tremula* L.) in Finland using airborne lidar and image data

Janne Toivonen[a,b], **Annika Kangas**[a], **Matti Maltamo**[b], **Mikko Kukkonen**[a], **and Petteri Packalen**[c]

[a]Natural Resources Institute Finland (Luke), Yliopistokatu 6, P.O. Box 111, Joensuu, FI-80100, Finland; [b]University of Eastern Finland (UEF), School of Forest Sciences, Yliopistokatu 7, P.O. Box 111, Joensuu, FI-80101, Finland; [c]Natural Resources Institute Finland (Luke), Latokartanonkaari 9, P.O. Box 2, Helsinki, FI-00791, Finland

Corresponding author: **Janne Toivonen** (email: janne.toivonen@luke.fi)

Abstract

European aspen is a keystone species in boreal forests, which support numerous ecologically important and endangered species. As detection of those species by remote sensing is impossible, we instead investigated the detection of large aspen trees using airborne laser scanning and aerial image data. However, this is a challenge due to their low quantity and scattered occurrence. The performance was assessed with representative and unrepresentative (where aspens were over-represented) samples of the population. First, we detected individual trees and then the random forest (RF) classifier was used to identify large aspens. The RF classification was implemented with and without synthetic minority oversampling technique (SMOTE) to balance the training data due to the rarity of large aspens. At the tree-level, the best F1-score (0.44) was obtained when the unrepresentative plot data were used with SMOTE. However, the F1-score decreased to 0.21 when the representative data were used. The best plot-level (plots with at least one aspen tree) F1-score with the representative plot data was 0.41. We conclude that although data augmentation may improve the result, it is difficult to detect large aspen trees in genuine populations.

Key words: airborne laser scanning, aspen, biodiversity, individual tree detection, random forest

1. Introduction

European aspen (*Populus tremula* L.) (hereafter aspen) is a keystone species and pioneer in boreal forests. Both living and dead aspen are important hosts for many forest-dwelling species, which include birds, fungi, invertebrates and mammals (Kouki et al. 2004; Kivinen et al. 2020). Numerous secondary hole-nesters, such as flying squirrels and tits also utilise aspen trees (Baroni et al. 2020). The ecological importance of the species is highlighted by the fact that many aspen-dependent species are also Red-listed species (Jonsell et al. 1998; Tikkanen et al. 2006), which means that the species is in danger of extinction (International Union for Conservation of Nature 2023). Old-growth, large-diameter (>20 or 25 cm) aspen trees are especially valuable from a biodiversity perspective (Latva-Karjanmaa et al. 2007; Maltamo and Packalen 2014). Aspen favours open areas for regeneration but is highly adaptive.

As a keystone species, there is a need for information on the abundance and occurrence of these trees at the landscape-level. This information is valuable in the planning and implementation of sustainable forest management and conservation. Also, a time series of aspen occurrence would provide valuable information on landscape health and integrity (Kay 1997). However, the number of aspen and other deciduous trees in boreal forests is limited due to traditional forest silviculture that has favoured coniferous trees, and also because natural disturbances rarely occur (Esseen et al. 1997; Kuuluvainen 2002). This type of information remains limited in northern Europe, although remote sensing technologies could bridge this information gap.

Current operative forest inventory methods employ a wide range of remote sensing data that range from optical images (aerial or satellite) to light detection and ranging (lidar) data (Maltamo and Packalen 2014; Næsset 2014). In the former, images contain information related to the emitted or reflected intensity of electromagnetic radiation. Lidar is an active remote sensing technology that can be spaceborne, airborne, or terrestrial. Airborne laser scanning (ALS or airborne lidar) is often utilised in 3D ecosystem assessments because these surveys provide valuable 3D information of the vegetation over large areas (Bakx et al. 2019). Forest inventory methods that use ALS data can be divided into two categories: area-based approach (e.g., Næsset 2002) or individual tree detection (e.g., Hyyppä et al. 2001). In the former, point cloud metrics are calculated at the plot- or raster cell-level and are used as predictor variables for stand attributes, while in the latter, the derivation of tree- or stand attributes is based on the prediction of tree dimensions from trees that are segmented from the ALS data. The required scale of information will determine the method used (Maltamo et al. 2014); for example, it may be desirable to detect dead standing trees or large aspen trees at the tree-level.

In recent years, ALS technologies have become increasingly popular in the fields of ecology, biodiversity, and conservation as they can characterise vertical and horizontal forest structures (Bergen et al. 2009; Davies and Asner 2014). Many studies have suggested that remote sensing information can serve as a relevant proxy for biodiversity and ecosystem assessment in vertically complex ecosystems, such as forests (Clawges et al. 2008; Bergen et al. 2009; Vihervaara et al. 2015; Toivonen et al. 2023). Earlier studies have highlighted the potential of 3D data for the mapping of aspen (Li et al. 2013;Alonzo et al. 2018). In addition, optical data (Erikson 2004; Alonzo et al. 2018) and unmanned aerial vehicle-based photogrammetric point clouds (Hardenbol et al. 2021; Kuzmin et al. 2021) have been reported to be effective for the detection of aspen, while the combined use of lidar and optical data for the detection of aspen and their attributes has also received attention (Säynäjoki et al. 2008; Breidenbach et al. 2010; Mäyrä et al. 2021). However, as large aspens are very rare and are easily mixed with surrounding broadleaved trees, their detection by remote sensing is a difficult task (Maltamo et al. 2015; Viinikka et al. 2020). Indeed, the research setup in previous studies has not always captured this important aspect. Moreover, the overlapping spectral response of aspen with other broadleaved trees, such as birch, is problematic (Korpela et al. 2010; Pippuri et al. 2013; Hovi et al. 2017), while the overlapping ALS-intensity properties of aspen and spruce have also been reported (Ørka et al. 2007).

The objective of this study was to evaluate the performance of the combined use of ALS data and aerial images for the detection of large aspen trees. The presence of aspens can be regarded as an indicator of important structure for forest biodiversity. Here, we define large aspen by its diameter at breast height (DBH), and our analyses are repeated across a range of DBH threshold values. The study was conducted with representative data at the population level, where the proportion of large aspen trees is very small, as is typical in Finnish forests. The performance of the investigated approaches was assessed by precision, recall and the F1 classification score. Our analyses evaluated how the classification performance varies when the rarity of large aspen trees in a forest stand is not properly considered in a research setting. This is demonstrated by repeating the analysis with an unrepresentative dataset, where the proportion of aspen is much greater than in natural forest environments.

2. Materials and methods

2.1. Study site

The study site is located in the south-boreal zone in eastern Finland and covers an area of approximately 3082 km^2 (Fig. 1). The rectangular shape of the study site was determined by the area covered by ALS data in the national data acquisition programme (Section 2.3). The main tree species in the study area are Scots Pine (*Pinus sylvestris* L.) and Norway spruce (*Picea abies* (L.) H. Karst). The most common deciduous tree species are silver birch (*Betula pendula* Roth) and downy birch (*Betula pubescens* Ehrh.). Other deciduous species, such as European aspen and grey alder (*Alnus incana* (L.) Moench), are in the minority. Most of the stands are mixed, i.e., there are multiple tree species in a stand.

2.2. Field data

Field data consisted of two types of field plots: National Forest Inventory (NFI) plots provided by Natural Resources Institute Finland (Luke) and treemap plots provided by the Finnish Forest Centre. The latter were measured in 2020 and 2021, whereas the NFI plots were measured between 2018 and 2021. To account for the obvious time lag, NFI trees from 2018, 2019, and 2020 were "extrapolated" to 2021 using internal (Luke) growth models (unpublished) based on NFI12 data (Korhonen et al. 2021). The sampling design of the Finnish NFI is explained in Korhonen et al. (2021). Treemap plots were subjectively placed within the study area as part of the operational stand-level forest management inventory.

Plot measurement protocols differed between the two plot types. In the NFI plots, all trees with DBH > 45 mm were measured in plots with a 9 m radius and smaller trees were measured in plots with either a 5.64 m (2018) or 4 m radius (after 2018). In the treemap plots, all trees with DBH > 30 mm were measured. Treemap plots were irregular in their shape and size (i.e., neither round nor rectangular). In the NFI plots, tree height was measured for sample trees and the heights of the other trees were predicted using the height model (model 18) proposed by Myllymäki (2016). In the treemap plots, the height of every fifth living tree was measured, and heights for trees clearly identifiable from ALS data were taken from the ALS data. For the remainder of the trees in the treemap plots, height was predicted separately for each tree species group with the height model described in Näslund (1937). Tree species information was recorded for both plot types. Tree locations were determined differently between plot types. In the NFI plots, location was included as a bearing and as the distance from the individual tree to the plot centre. In the treemap plots, locations had been determined by the Finnish Forest Centre using the TerraHärp system implemented with Masser ExCaliper II callipers (Kostensalo et al. 2023).

Tree measurements were harmonised by only selecting trees that had DBH values > 45 mm. For the analysis, we primarily used measured tree height as tree height, but where that data were not available, we used the abovementioned height model based predicted height. We also had to account for the differences in the shapes of the two types of plot data. As the shape of treemap plots varied and were considerably larger than the NFI plots, we placed a 9 m radius sub-plot within each treemap plot to create a corresponding 9 m radius circular plot (as in the NFI). Each sub-plot was located as the centre of each treemap plot as much as possible. Trees recorded inside these sub-plots were used in the analyses.

In total, there were 33 195 field-measured trees distributed across 701 plots, which included both NFI and treemap subplots. The number of deciduous trees other than aspen was 9079, which corresponded to 27.4% of the trees in the field data. There were only 167 aspen trees in the dataset, which corresponded to 0.5% of all field-measured trees. Of those, 35 aspen trees had DBH values ≥ 22 cm, which corresponded

Fig. 1. Location of the aspen study site and the remote sensing (RS) and field (treemap plots and Finnish National Forest Inventory (NFI) plots) data used. Figs was created using QGIS version 3.34.3 and assembled from the following data sources: clipped map of Northern Europe (Esri World Countries Generalized) and a large background aerial image (National Land Survey of Finland).

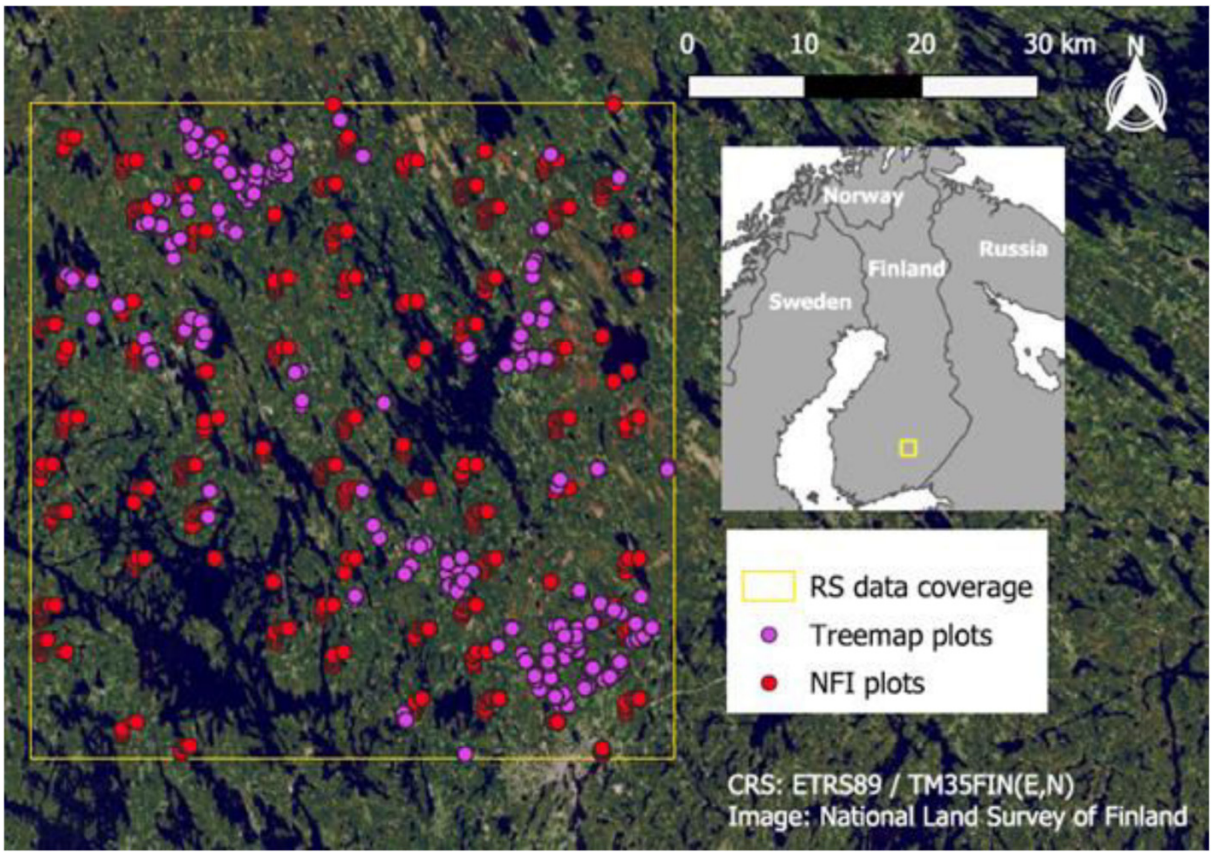

to 1.96 large (DBH ≥ 22 cm) aspen per hectare. The corresponding mean estimate in the NFI for the larger Etelä-Savo region in which the study site was located, is 2.21 large aspen per hectare (DBH ≥ 22 cm, computed specifically for this study using NFI data between 2019 and 2021). The diameter distributions of aspen and other trees in the field data are displayed in Fig. 2, where the left-hand side *y*-axis indicates the absolute number of aspen (bars) and the right-hand side *y*-axis indicates the number of other trees (displayed as a smoothed red line). The shape of the diameter distribution of aspen approximately follows the diameter distribution of the other trees (Fig. 2).

2.3. Remote sensing data

Remote sensing data consisted of ALS data and aerial images. Both datasets are part of the national data collection campaign (KALLIO) organised by the National Land Survey of Finland and are freely available, although some restrictions apply to the acquisition of high-density ALS data. The ALS data and aerial images were acquired during leaf-on conditions in June 2020 (Tables 1 and 2). As proposed by Axelsson (2000), the ALS echoes were classified as ground and non-ground. The original echo heights in the N2000 vertical coordinate reference system were normalised to above ground level (a.g.l) using a digital terrain model interpolated from ground echoes by Delaunay triangulation. Resulting negative echo heights were set to zero.

We used the original multispectral bands (Level-2) from a Vexcel UltraCam Eagle camera, without pan-sharpening or orthorectification. Pan-images were not used. First of many and only echoes were projected to unrectified colour bands using the parameters of internal and external orientation (see details in Packalén et al. 2009). External orientation was determined using the bundle block adjustment technique with tie points, control points, and GNSS (global navigation satellite system) IMU (inertial measurement unit) values as ancillary observations (Mikhail et al. 2001). The pixel values of the colour bands (red, green, blue, and near-infrared (NIR)) were then assigned as attributes to the ALS echoes. Note: Due to the overlap of images, each ALS echo was linked to multiple images.

2.4. Tree detection and tree metrics

Trees were identified from the canopy height model (CHM) interpolated by the ground normalised ALS echoes. The pixel size of the CHM was 0.5 m and the initial CHM was interpolated by setting the pixel value either to the maximum ALS echo height within each pixel or as NoData (if there were no

Fig. 2. Histogram for the diameter distribution of aspen (bars) and other trees (smoothed red line) used in this study. Each bar equates to the 3 cm diameter at breast height class.

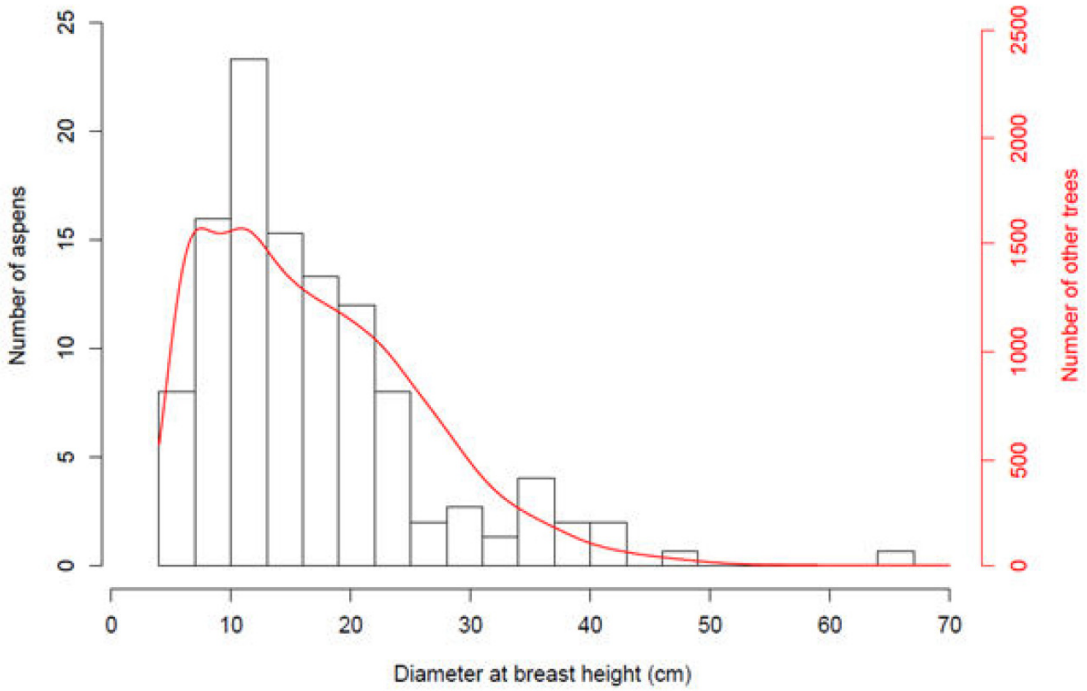

Table 1. Metadata of the applied airborne laser scanning data used to detect aspen in this study.

Time	14 June 2020–25 June 2020
Laser scanner	RIEGL VQ-1560i
Flying altitude	1525 m a.g.l.
Flying speed	155 knots
Scanning frequency	148 Hz
Pulse density	1400 kHz
Point density	7.2 points/m2
Maximum scanning angle	20°
Side overlap	20.8%

Table 2. Metadata of the aerial images used in aspen detection.

Time	12 June 2020
Multispectral Camera	Vexcel UltraCam Eagle Mk.*
Image format, mm	68.016 × 104.052
Image format, pixels	4360 × 6670
Pixel size (in CCD)	15.600 μm × 15.600 μm
Focal length	100.5 mm
Spectral bands (FWHM*)	Red: 580–690 nm
	Green: 490–580 nm
	Blue: 420–500 nm
	NIR: 690–880 nm
Flying altitude	7700 m a.g.l.
Flying speed	257 knots
Ground sampling distance of multispectral camera	120 cm

*Full width at half maximum.

ALS echoes within a pixel). NoData pixels were then replaced with the median value in a 3 × 3 neighbourhood, and this was repeated until no NoData pixels remained. After that, a pixel was considered as a pit if at least six of its neighbours in the 8-neighbourhood were >5 m higher than the pixel itself. These pit pixels were replaced with the median values of their neighbourhood. The CHM was low-pass filtered using a Gaussian kernel and the magnitude of low-pass filtering was determined by the value of a sigma (σ) parameter. After preliminary testing, we used a σ value of 1.2 (in pixel coordinates).

Tree tops were identified from the low-pass filtered CHM by assuming that the local maximum in the 8-neighbourhood corresponded to a tree. Trees were delineated from the CHM using marker-controlled watershed segmentation with identified treetops as seeds. Watershed segments were delineated using a drainage direction following an algorithm (Narendra and Goldberg 1980; Gauch 1999) within the inverted (low-pass filtered) CHM. To maintain separation between the crown and ground, pixels with heights of <5 m were excluded. Finally, tree segments with a crown size < 3 m^2 or a local maximum height < 14 m were removed. Note: Tree detection parameters were selected to detect large aspen rather than for generic forest inventory purposes.

Field measured trees were linked to remotely detected trees to attach the information related to a field tree (here DBH and tree species) to the detected tree (Fig. 3). As a linking criterion, we used a 2.5 m limit in the X and Y planes, and a 3 m limit in the Z direction. If multiple trees were found within these limits, the nearest tree was selected. This linking resulted in 12 189 linked trees.

Fig. 3. Workflow for the classification of large aspen trees.

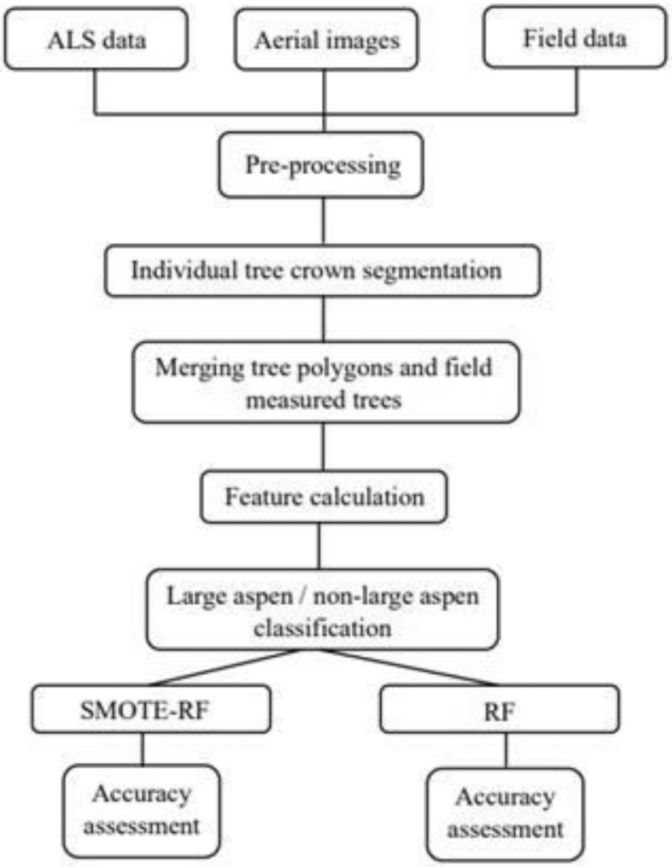

The ALS and image metrics were calculated for the CHM segmented tree polygons. The ALS metrics were calculated for the first, intermediate, last and all echo categories and included commonly used height and intensity percentiles (5th, 10th, …100th) for echoes ≥ 2 m a.g.l. Also, we calculated the proportion of the different echo categories, mean, standard deviation, skewness, and kurtosis for height and intensity. Density metrics (e.g., D15 and D20) were calculated as cumulative proportions of echoes above certain heights (e.g., 15 and 20 m). Image metrics, which contained mean and standard deviation values for each band, ratios between the bands (e.g., red/blue) and normalised difference vegetation index (NDVI), were computed for trees from the pixel values linked to echoes. Only echoes with a height > 0.5 × the predicted height of the tree were accepted. For this purpose, tree height was predicted for detected trees using a linear model fitted with all the detected and appropriately linked trees. In the model, the maximum height of the remotely sensed tree polygon (*hPoly*) explained the measured/predicted height of the tree (*hTree*):

$$(1) \qquad hTree_i = \beta_0 + \beta_1 \times hPoly_i$$

where β_0 is a constant in the model and β_1 is the coefficient of the model. Model coefficients were estimated using the least squares method, which resulted in values of 1.24 for β_0 and 1.00 for β_1 (i.e., only the intercept was required at the end).

2.5. Classification of aspen trees

We used the random forest (RF) classifier to separate large aspen from other remotely detected trees (Fig. 3). The RF classifier is a well-established algorithm in data science and has been widely used in remote sensing (Belgiu and Drăguţ 2016). It is a supervised learning method that constructs multiple decision trees at the training stage. Each decision tree consists of nodes that are chosen based on optimum splitting of features. In our analysis, we used Gini importance (a.k.a. Gini impurity) as a node splitting criterion. Output of the algorithm is the class selected by most of the trees, i.e., majority voting. We used the "fast implementation of random forest algorithm" from package ranger (Wright and Ziegler 2017) in the R environment (R Core Team 2022).

Our dataset was strongly unbalanced as the proportion of large aspen was very small compared to other trees (e.g., 35 aspen with DBH > 22 cm from a total of 33 195 trees). Also, the number of aspen was small compared to other deciduous trees; aspens comprised approximately 1.8% of all deciduous trees (167 aspens from a total of 9246 deciduous trees). To account for the imbalance, we adopted the synthetic minority oversampling technique (SMOTE) (Chawla et al. 2011) where new instances are generated by combining features of the target observation and its k-nearest neighbours in the feature space. The user defined parameters of SMOTE are the percentages for minority case increment and/or majority decrement and the number of nearest neighbours. For example, if one wants to double the number of minority observations, the percentage for minority increment is 200. In our analysis, we calculated values for minority increment in such a way that the numbers of aspen and other tree species in the training data were approximately equal. For example, a total of 7627 trees were used in the modelling when the 22 cm DBH limit for large aspen was applied, and only 29 of these were large aspen. The use of SMOTE increased the number of large aspens to 7598 in the training data while the number of other trees remained unchanged. This also corresponded better to the number of other deciduous trees in the field data. We used SMOTE implemented in the R-package performanceEstimation (Torgo 2016).

Initially, there were 179 ALS and 15 image metrics. Prior to fitting the RF model, we removed ALS metrics until the correlations between the remaining metrics were <0.8. All image metrics were used as there were significantly more ALS metrics than image metrics. For the response class "large aspen," we defined those observations that were aspen and where DBH was ≥a range of DBH limits (18, 20, 22, 24, and 26 cm). The definition of large aspen may be ambiguous, as earlier studies have used DBH values between 20 and 25 cm as a criterion (e.g., Latva-Karjanmaa et al. 2007; Maltamo et al. 2015).

Our first classification (SC1) compared balanced (SMOTE-RF; SRF) and unbalanced RF classifications, when the 22 cm DBH limit for large aspen was used. In SC1, the data were divided into A, B, and C datasets for both balanced and unbalanced classifications. Dataset A denoted data where only linked trees (i.e., trees for which tree polygons were assigned) from the aspen plots were considered. Here, aspen plot indicates that the plot contained at least one large aspen tree. In

Table 3. Confusion matrices associated with our first classification (SC1) where the random forest (RF) algorithm and synthetic minority oversampling technique augmented RF classification (SMOTE-RF) were compared across different datasets. Labels "Aspen" and "Other" denote large aspens and other trees, respectively. Suffix "A" denotes the dataset where only linked trees from aspen plots were considered, suffix "B" denotes the dataset where unlinked field-measured trees from aspen plots were added to previous results, and suffix "C" denotes the dataset where all trees from all plots were used in the classification.

		Observed class				Observed class		
	RF-A	Other	Aspen	Sum	SRF-A	Other	Aspen	Sum
Predicted class	Other	**430**	19	449	Other	**409**	13	422
	Aspen	8	**10**	18	Aspen	29	**16**	45
	Sum	438	29	**467**	Sum	438	29	**467**
	RF-B	Other	Aspen	Sum	SRF-B	Other	Aspen	Sum
Predicted class	Other	**1371**	25	1396	Other	**1350**	19	1369
	Aspen	8	**10**	18	Aspen	29	**16**	45
	Sum	1379	35	**1414**	Sum	1379	35	**1414**
	RF-C	Other	Aspen	Sum	SRF-C	Other	Aspen	Sum
Predicted class	Other	**33 159**	34	33193	Other	**33 136**	28	33164
	Aspen	1	**1**	2	Aspen	24	**7**	31
	Sum	33160	35	**33195**	Sum	33160	35	**33 195**

dataset B, unlinked field measured trees from the aspen plots were added to the data, while in dataset C, all trees from all plots were considered in the classification. Dataset C was representative of the population, while A and B were unrepresentative. Our second classification (SC2) compared SMOTE-RF classifications across a range of DBH limits for large aspen (18, 20, 22, 24, and 26 cm).

We utilised the leave-one-plot-out cross-validation technique, which means that for each iteration, we used trees from one plot as the test data and trees from all the other plots as the training data. We report the following accuracy statistics: precision, recall, and the F1-score. The latter is a harmonic mean value of precision and recall (Sasaki 2007). In SC1, we report tree-level accuracies for aspen plots (A, B) and all plots (C). In SC2, we show accuracies only for all plots, but the results are reported at both the tree- and plot-levels.

Finally, we analysed the most important metrics used in the SMOTE-RF classification at the 22 cm DBH limit when data from aspen plots and all plots were utilised. The importance measure employed here was the decrease in Gini importance, which is calculated as the number of times that a metric is used to split a tree node divided by the number of all trees. The importance measure values across RF runs with different datasets are at different scales. To make them comparable (between the aspen plots and all plots), we normalised importance by dividing it by its overall mean value.

3. Results

In SC1 (22 cm DBH limit), 29 large aspens were linked to remotely detected tree crowns. In addition, six large aspens were not linked to a remotely detected tree. Therefore, the total number of large aspen in SC1 was 35. In the aspen plots, we were able to identify 10 large aspens (out of 29) with the RF method (Table 3, RF-A) and 16 out of 29 with the SMOTE-RF method (Table 3, SRF-A). When all 701 plots were used, the number of correctly identified large aspen trees was 1 and 7 (out of a total of 35) with the RF and SMOTE-RF methods, respectively.

Table 4. Accuracy statistics associated with our first classification (SC1) where the random forest (RF) algorithm and synthetic minority oversampling technique augmented RF classification (SMOTE-RF) were compared across different datasets.

	Precision	Recall	F1-score
RF-A	0.56	0.34	0.42
SRF-A	0.36	0.55	0.44
RF-B	0.56	0.29	0.38
SRF-B	0.36	0.46	0.40
RF-C	0.50	0.03	0.06
SRF-C	0.23	0.20	0.21

The accuracy statistics for SC1 are shown in Table 4. The F1-scores for dataset A were similar (0.42 vs. 0.44) because a considerable number of large aspens were incorrectly predicted in SMOTE-RF. This difference was also seen in the smaller precision values associated with SMOTE-RF, which indicated a greater proportion of incorrectly predicted aspens. The recall values were greater for SMOTE-RF than for RF, i.e., the predicted large aspens were more often correct in SMOTE-RF than in RF. The accuracy statistics for dataset B highlighted the errors that originated from the unlinked field-measured trees (Table 4, RF-B, SRF-B). The recall values for dataset B with RF and SMOTE-RF classification were 0.05 and 0.09 smaller, respectively, than in dataset A. The F1-scores for both classifications were 0.04 smaller than dataset A. The difference in the statistics with dataset A remained relatively small as

Table 5. Confusion matrices associated with our second classification (SC2) where synthetic minority oversampling technique augmented RF classification (SMOTE-RF) was used to identify large aspens across a range of diameter at breast height limits at the tree- and plot-levels. Labels "Aspen" and "Other" at the tree-level denote large aspen trees and other trees, respectively. At the plot-level, these correspond to non-large aspen plots and large aspen plots.

		Tree-level				Plot-level		
	18 cm	Observed class			18 cm	Observed class		
		Other	Aspen	Sum		Other	Aspen	Sum
Predicted class	Other	**33 085**	58	33143	Other	**641**	24	665
	Aspen	46	**6**	52	Aspen	27	**9**	36
	Sum	33131	64	**33 195**	Sum	668	33	**701**
	20 cm				20 cm			
		Other	Aspen	Sum		Other	Aspen	Sum
Predicted class	Other	**33 114**	44	33158	Other	**653**	22	675
	Aspen	32	**5**	37	Aspen	19	**7**	26
	Sum	33146	49	**33 195**	Sum	672	29	**701**
	22 cm				22 cm			
		Other	Aspen	Sum		Other	Aspen	Sum
Predicted class	Other	**33 136**	28	33164	Other	**662**	16	678
	Aspen	24	**7**	31	Aspen	15	**8**	23
	Sum	33160	35	**33195**	Sum	677	24	**701**
	24 cm				24 cm			
		Other	Aspen	Sum		Other	Aspen	Sum
Predicted class	Other	**33 157**	19	33176	Other	**674**	13	687
	Aspen	12	**7**	19	Aspen	7	**7**	14
	Sum	33169	26	**33 195**	Sum	681	20	**701**
	26 cm				26 cm			
		Other	Aspen	Sum		Other	Aspen	Sum
Predicted class	Other	**33160**	15	33175	Other	**673**	10	683
	Aspen	13	**7**	20	Aspen	11	**7**	18
	Sum	33173	22	**33 195**	Sum	684	17	**701**

most of the field-measured trees were non-aspen trees and we were able to link most of our field measured large aspen to a remotely detected tree. Precision values remained similar as the unlinked field-measured trees mostly belonged to the "Other" class.

The advantage of SMOTE-RF was evident when all plots were considered (Tables 3 and 4, dataset C). SMOTE-RF resulted in a clearly greater F1-score than RF: 0.21 versus 0.06 (Table 4). Moreover, SMOTE-RF also predicted a greater number of large aspens, although many were incorrectly predicted (precision 0.23). In contrast, RF predicted only two large aspens, and only one was correct (Table 3). Further inspection on the tree species distribution of false positives in SRF-C revealed that most of the false positives (20 trees out of 24) were birch trees (silver birch and downy birch), three were spruce and one was pine.

Confusion matrices associated with SC2 are presented in Table 5, and Fig. 4 depicts the F1-score, precision and recall values for SC2. All the results are shown for a range of DBH limits at the tree- and plot-levels. The total number of large aspen trees in our dataset strongly declined when the DBH limit increased from 18 cm ($n = 64$) to 26 cm ($n = 22$) (Table 5). At the tree-level, the number of correctly classified aspens was approximately similar (5–7) across a range of DBH limits (Table 5). Tree-level F1-scores increased as the DBH limit increased (Fig. 4A). The same trend applied with the precision (Fig. 4B) and recall values (Fig. 4C), with the exception that the precision value was greatest at the 24 cm DBH limit. At the plot-level, the number of correctly classified aspen plots remained approximately similar, although the number of aspen plots declined from the DBH limit of 18 cm ($n = 33$) to 26 cm ($n = 17$) (Table 5). The F1-scores increased overall with increasing DBH, although the 24 cm limit had greater precision than the 26 cm limit (Fig. 4A). Precision exhibited the same trend as the F1-score; the 24 cm limit exhibited the greatest F1-score (0.50) followed by the 26 cm limit (0.39)

Fig. 4. Plot- and tree-level F1-scores (A), precision (B), and recall values (C) associated with our second classification (SC2) where the synthetic minority oversampling technique augmented RF classification (SMOTE-RF) was used to identify large aspen trees across a range of diameter at breast height (DBH) limits at the tree- and plot-levels.

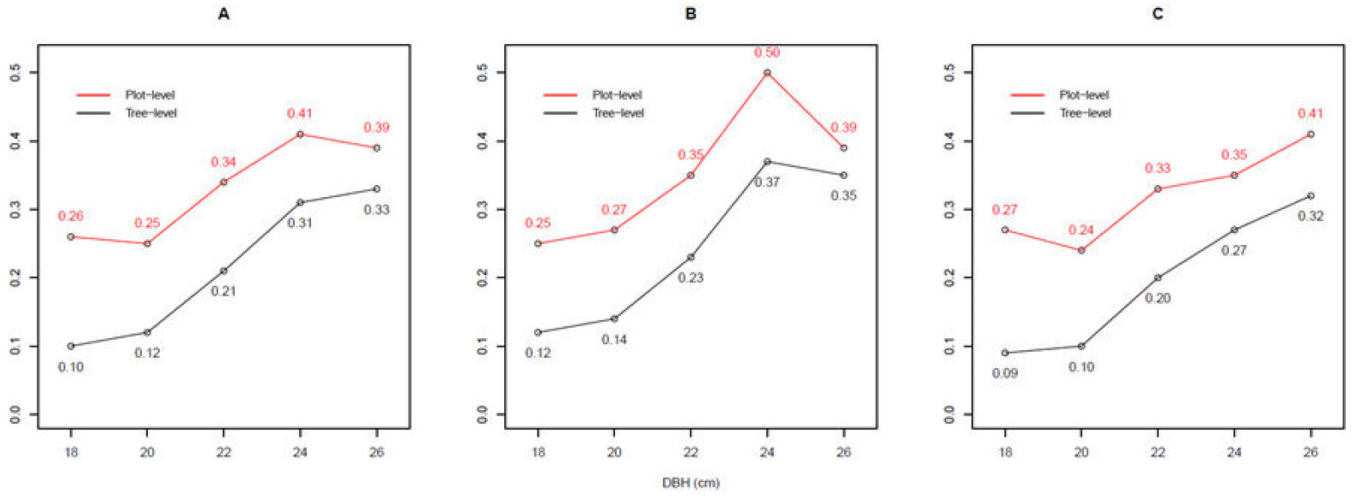

(Fig. 4B). Recall values showed a similar trend (Fig. 4C). All accuracy statistics at the plot-level exhibited greater values than their equivalents at the tree-level.

Normalised importance of the 20 most important ALS and aerial image metrics for the two selected datasets are presented in Fig. 5. These correspond to previously reported datasets SRF-B and SRF-C in SC1. Overall, image metrics were clearly more important predictors than ALS metrics (Fig. 5). In particular, metrics that contained the NIR band were considered to be very important. NDVI also exhibited high importance values for both datasets. The green band appeared to be the second most important spectral band. The most important ALS metric was ranked 8th in importance with the aspen plots and 12th with all plots (Fig. 5). The most important ALS metrics listed here were related to lidar intensity (e.g., f_int5 = 5th intensity percentile of the first of many + only echoes).

4. Discussion

The low accuracy statistics reported in this study highlight the challenges in remote-sensing-based detection of aspen in large forest areas with diverse conservation and management targets. This was seen in SC1 as the highest F1-scores were reported for the least representative dataset of the population, whereas the lowest F1-scores were reported with the most representative dataset of the population. SC1 also showed that data augmentation using SMOTE was beneficial for the most representative dataset, although accuracies were still poor. In SC2, the number of correctly classified large aspens varied slightly when different DBH limits were applied. Further inspection revealed that the same four large aspen trees were correctly identified for all DBH limits, and six correctly classified large aspen trees were the same for the 22, 24, and 26 cm DBH limits. One possible reason that the same large aspen trees were correctly identified was that their structure and/or spectral response were clearly different to the surrounding trees in the same plot. This confirms that large aspens are, to some extent, identifiable via remote sensing.

From a biodiversity point of view, it is meaningful to identify large aspen trees, whether clustered or few and far between. Therefore, the basic unit of interest in our study was the tree, and quantities were considered as less important. In addition, we wanted to validate the classification accuracy (absence or presence of large aspen) at the plot-level, which was based on the predictions at the tree-level in each plot. Stand-level assessment would have also been of interest, but we did not have data for such an analysis. Tree- and plot-level results were reported in SC2, where the plot-level accuracy was greater than tree-level accuracy at each DBH limit. This is an assumed outcome because we applied a chain of reasoning that allowed aspen plots to be predicted, even though there were no observed large aspens in that plot. For example, a plot would still be classified as an aspen plot if a single large aspen was predicted, regardless of whether the prediction was correct or incorrect.

Our study setting provides a realistic picture of the difficulty in modelling rare phenomena in true populations. In our field data, the proportion of aspen with respect to stem number was 0.49%, while the corresponding mean estimate in the Finnish NFI for the larger geographical area that surrounds our study area is 0.5% (computed specifically for this study using NFI data collected between 2019 and 2021). The proportion of large aspens in our study area is much smaller, around 0.1% for aspen with a DBH $\geq$ 22 cm. This rarity of aspen in the population has not been adequately taken into account in earlier research setups. For example, the proportion of aspen in the studies by Viinikka et al. (2020) and Mäyrä et al. (2021) was approximately 11%, and 27% in the study by Kuzmin et al. (2021).

The overlapping spectral response between birch and aspen is a known issue in the identification of the latter (e.g., Hovi et al. 2017; Viinikka et al. 2020). As such, our

Fig. 5. Normalised importance for the 20 best remote sensing metrics used in the synthetic minority oversampling technique augmented RF (SMOTE-RF) classification at the 22 cm diameter at breast height limit. Black and grey colours signify spectral and airborne laser scanning metrics, respectively. A greater value signifies greater importance. Definitions: f—first and only echoes, l—last and only echoes, i—intermediate echoes, a—all echoes, int—intensity metric, std—standard deviation, h—height percentile (e.g., h5 = 5th height percentile), echo_prop—proportion of echo class from all echoes, hkurt—kurtosis (4th moment) of vegetation heights, NDVI—normalised difference vegetation index, NIR—near-infrared,/– division of two image bands.

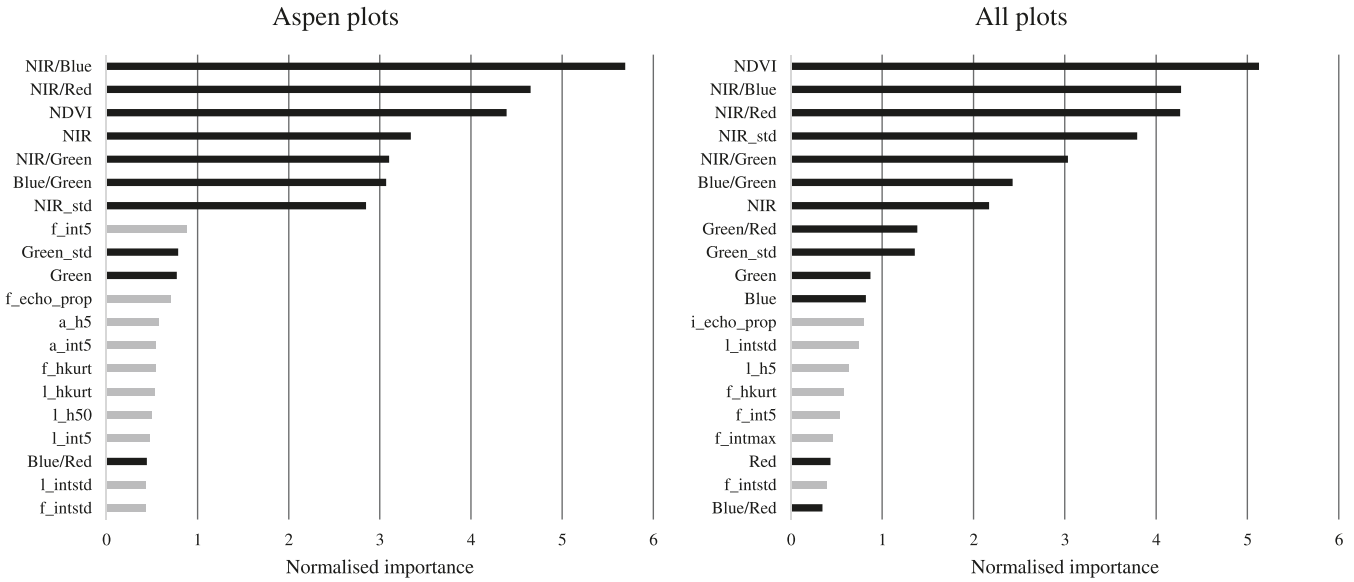

investigation of tree species distribution of false positives in classification SRF-C in SC1 revealed that most of the falsely predicted large aspens were actually birch trees: 20 out of a total of 24. Of the remainder, three were spruce and one was pine. Therefore, our study underlines the misclassification issue between aspen and birch. Other causes for misclassification between aspen and other deciduous trees are similarities in tree structure and high chlorophyll content (Dalponte et al. 2012).

Comparison of our results to other studies is difficult due to the number of factors involved, including the proportion of aspen in the dataset, the number of other species, the difference in overall vegetation structure, and the season of data acquisition. In addition, our interest was specifically in large aspen, not aspen in general. Kivinen et al. (2020) reviewed remote sensing-based mapping of aspen at the tree- and stand-levels and listed various studies in which the precision varied between 0.56 and 0.86, and recall values ranged between 0.24 and 0.71. One of those tree-level studies was Ørka et al. (2007), who utilised ALS intensity features in tree species classification in a natural forest reserve in Norway. The proportion of aspen in their field data were 9.4% of all trees and approximately 23% of deciduous trees. They reported relatively low classification accuracies for aspen; a precision value of 0.56 and a recall value of 0.24. They also noted that there was overlap between aspen and spruce ALS intensity metrics, which was also reported by Korpela et al. (2010). These accuracy statistics are somewhat similar to the results presented here, although the aspens in our study were more often mixed with birch trees than with spruce.

In Koli National Park in eastern Finland, Säynäjoki et al. (2008) utilised ALS data, combined with aerial images, to separate aspen from other deciduous trees. First, they visually discriminated deciduous trees from coniferous trees using aerial images. Second, ALS data were employed to classify the remaining segments as aspen and other deciduous trees with 79% accuracy. One explanation for the greater accuracy compared to our study is that they utilised manual segmentation of tree crowns in the first stage. This procedure simplifies classification by reducing the amount of confounding tree delineations. However, this approach is not realistic in real world applications. Moreover, they recorded a large number of aspen trees (n = 140) compared to other deciduous trees (n = 56) in their dataset. This was opposite to our dataset where the proportion of aspens from all deciduous trees was only 1.8%.

Li et al. (2013) utilised very high-density ALS data (90 points/m^2) to classify individual tree crowns into four species, one of which was quaking aspen (*P. tremuloides* Michx.). The proportion of aspen in their field data was over 30% of all trees and approximately 63% of deciduous trees, and they recorded high precision (0.74) and recall (0.76) values. They reported that the high ALS point density strongly contributed to the classification accuracy. In Finland, Viinikka et al. (2020) and Mäyrä et al. (2021) tested the performance of airborne hyperspectral data for the detection of aspen at the same study site. They only utilised ALS data for the detection of individual tree crowns. In the former study, the main emphasis was on finding the most important spectral features for the discrimination of aspen from the other tree species, but also to

compare the RF and support vector machine classifiers. The latter study concentrated more on a comparison of the different classifiers used in the identification of aspen. Both studies reported similar accuracies for their best performing models: a precision value of approximately 0.93 and a recall value of approximately 0.89. Compared to our study, both Viinikka et al. (2020) and Mäyrä et al. (2021) had a clearly greater proportion of aspen in their field data. Also, the proportion of aspens with regard to other deciduous trees was also clearly greater in their field data (36.1% vs. 1.8%).

Unmanned aerial system (UAS)-based mapping of aspen trees has been reported to result in similar accuracies as studies that have utilised conventional ALS data and multispectral aerial images. For example, Tuominen et al. (2018) studied the recognition of 26 tree species (2.8% aspen) in a Finnish arboretum using UAS hyperspectral and 3D point cloud data. They utilised manual delineation of tree crowns and reported a precision value of 0.86 and a recall value of 0.63 for aspen classification. Kuzmin et al. (2021) examined the mapping of aspen trees using multispectral UAS point cloud data. The best feature set obtained a precision value of 0.82 and a recall value of 0.85 in a two-class scenario. Hardenbol et al. (2021) utilised spectral and height information from UAS 3D point clouds and reported precision values between 0.84 and 0.97 and recall values between 0.84 and 0.96 for different dates of data acquisition. These studies reported much greater values for accuracy statistics than in our study. A potential reason for this is that study of Tuominen et al. (2018) was conducted in an arboretum that had homogeneous stands, which made them suitable for tree species recognition. In the studies of Hardenbol et al. (2021) and Kuzmin et al. (2021), the proportion of aspen in the field data was clearly greater than in our data: 20.7% and 29.4% of all trees, and 39.8% and 54.5% of deciduous trees, respectively. Furthermore, Hardenbol et al. (2021) visually selected coniferous trees (spruce and pine) for the classification, which might have made the classification between aspen and other tree species easier.

In our study, the NIR band, the band ratios of NIR and other bands, and NDVI were the most important metrics in the detection of large aspen trees. Earlier studies have reported similar findings with regard to the NIR band (e.g., Viinikka et al. 2020). Hardenbol et al. (2021) suggested that the most favourable time window for the detection of aspen was late spring when aspen did not have leaves and birch had only partially flushed leaves. Summer was considered the second best and autumn the least favourable time. In operational applications, it is not practical to collect data in short time periods only in spring or autumn. Our remote sensing data were collected in summertime when the leaves were fully opened. The importance of NDVI has also been recognised in other studies (e.g., Hardenbol et al. 2021).

Our results show that spectral metrics are more important than ALS metrics for the classification of large aspen. This is in line with the observations of Hardenbol et al. (2021) where only one height metric (45th percentile of vegetation heights, h45) was selected in the final model and had a comparatively small effect in the classification. However, the most important ALS metrics in our study were related to echo intensities (e.g., f_int5 and l_intstd). The wavelength of the used ALS instrument is 1064 nm, which provides intensity values that perform well in the separation of tree species (see e.g., Korpela et al. 2023). Ørka et al. (2007) reported similar findings and noted that the best performing combination of predictors included mean intensity values and associated standard deviation computed either from first or last echoes. Our results underline this finding, as the standard deviation values associated with intensity either from last or first echoes were included in the 20 most important metrics.

The optimal tuning parameters for the detection of large aspens deviate from the parameters used in generic forest inventories and are unfavourable for the detection of small trees. One reason is the magnitude of the low-pass filtering that is required for large-crowned aspen trees to have only one local maximum. Here, we do not present the effect of the tree detection parameters. These parameters have a certain effect, but because there are multiple tree detection algorithms, all with different tuning parameters, such an analysis is not particularly useful. An issue related to delineation of tree crowns in our study was the fact that our field data contained many plots that had a multilayered canopy structure and were, therefore, problematic for individual tree detection. In earlier studies, manual delineation of tree crowns resulted in greater detection accuracies for aspen than obtained from automatic delineation (Hardenbol et al. 2021). Nevertheless, the use of manual delineation in real world applications is not a realistic option (Tuominen et al. 2018).

For future studies, we recommend that more resources are allocated to the detection of ecologically valuable trees, such as large aspen. One problem in separating aspen from other deciduous trees are the subtle differences in the crown shape, structure, and spectral response. It is obvious that the crown shape of aspen is such that the assumption of one local maximum at the top of a tree is not always realistic. More emphasis is required to tackle the issue of mixing between aspen and other deciduous trees. Furthermore, future studies should pay more attention that the used dataset is representative with respect to population, and if it is not, to state this clearly and discuss its implications in a transparent manner.

5. Conclusion

We demonstrated here that both the rarity of large aspen trees and their mixing with surrounding broadleaved trees, especially birch, make their detection with ALS data and aerial images a difficult task in a genuine population. This aspect of rarity has not been properly considered in earlier studies and was, therefore, demonstrated here by repeating the analyses with representative (proportion of aspen is similar in the population) and unrepresentative (proportion of aspen is noticeably greater than in the population in the large area) datasets. Performance was clearly poorer in the representative dataset, which means that overly optimistic results may occur in studies where the validation data contain more large aspen trees than are in the population. Our results showed improved performance with SMOTE, which indicates that data augmentation may be beneficial for the mapping of rare phenomena, such as large aspen trees. With regard to the classification accuracy related to the size of

aspen trees, we observed that an increased DBH limit for "large aspen" improved the classification accuracy. The spectral metrics were found to be more important predictors than the ALS metrics when separating identified individual trees. However, ALS metrics may further improve the accuracy, and in our approach, ALS data are also required for the detection of trees.

We underline the fact that large aspen trees have such a crown structure that the assumption of one local maximum at the treetop is not relevant. This provides space for the development of a dedicated approach that is tailored to the detection of the crown of large aspen trees. Future studies should use field data that provides the most realistic picture of the surrounding forest landscape.

Acknowledgements

We thank the Kone Foundation for partly funding this study and previous paper of my (Janne Toivonen, corresponding author) DSc under the grant agreement No. 202201370.

Article information

History dates

Received: 20 November 2023
Accepted: 14 February 2024
Accepted manuscript online: 22 February 2024
Version of record online: 30 May 2024

Copyright

Data availability

Data generated or analysed during this study are not available due to the nature of this research. Finnish NFI plots (Luke) and treemap plots (Finnish Forest Centre) are not publicly available. ALS data and aerial images are publicly available at: https://asiointi.maanmittauslaitos.fi/karttapaikka/tiedostopalvelu.

Author information

Author ORCIDs

Janne Toivonen https://orcid.org/0000-0003-1319-3035
Annika Kangas https://orcid.org/0000-0002-8637-5668
Matti Maltamo https://orcid.org/0000-0002-9904-3371
Mikko Kukkonen https://orcid.org/0000-0003-4206-1680
Petteri Packalen https://orcid.org/0000-0003-1804-0011

Author contributions

Conceptualization: JT, PP
Data curation: JT
Formal analysis: JT
Investigation: JT
Methodology: JT, PP
Project administration: PP
Resources: JT, PP
Software: JT, PP
Supervision: AK, MM, MK, PP
Validation: JT, AK, MM, MK, PP
Visualization: JT
Writing – original draft: JT, AK, MM, MK, PP
Writing – review & editing: JT, AK, MM, MK, PP

Competing interests

The authors declare there are no competing interests.

Funding information

This study was supported by the Research Council of Finland fundings 323484, 337127, and 337655, and Kone Foundation funding 202201370.

References

Alonzo, M., Andersen, H.E., Morton, D.C., and Cook, B.D. 2018. Quantifying boreal forest structure and composition using UAV structure from motion. Forests, **9**: 119. doi:10.3390/f9030119.

Axelsson, P., 2000. DEM generation from laser scanner data using adaptive TIN models. Int. Arch. Photogramm. Remote Sens. **33**: 110–117.

Bakx, T.R.M., Koma, Z., Seijmonsbergen, A.C., and Kissling, W.D. 2019. Use and categorization of light detection and ranging vegetation metrics in avian diversity and species distribution research. Divers. Distrib. **25**(7): 1045–1059. doi:10.1111/ddi.12915.

Baroni, D., Korpimäki, E., Selonen, V., and Laaksonen, T., 2020. Tree cavity abundance and beyond: nesting and food storing sites of the pygmy owl in managed boreal forests. For. Ecol. Manage. **460**: 117818. doi:10.1016/j.foreco.2019.117818.

Belgiu, M., and Drăguţ, L. 2016. Random forest in remote sensing: a review of applications and future directions. ISPRS J. Photogramm. Remote Sens. **114**: 24–31. doi:10.1016/j.isprsjprs.2016.01.011.

Bergen, K.M., Goetz, S.J., Dubayah, R.O., Henebry, G.M., Hunsaker, C.T., Imhoff, M.L., et al. 2009. Remote sensing of vegetation 3-D structure for biodiversity and habitat: review and implications for lidar and radar spaceborne missions. J. Geophys. Res. Biogeosci. **114**(G2). doi:10.1029/2008JG000883.

Breidenbach, J., Næsset, E., Lien, V., Gobakken, T., and Solberg, S. 2010. Prediction of species specific forest inventory attributes using a nonparametric semi-individual tree crown approach based on fused airborne laser scanning and multispectral data. Remote Sens. Environ. **114**(4): 911–924. doi:10.1016/j.rse.2009.12.004.

Chawla, N.V., Bowyer, K.W., Hall, L.O., and Kegelmeyer, W.P. 2011. SMOTE: synthetic minority over-sampling technique. J. Artif. Intell. Res. **16**: 321–357. doi:10.1613/jair.953.

Clawges, R., Vierling, K., Vierling, L., and Rowell, E. 2008. The use of airborne LiDAR to assess avian species diversity, density, and occurrence in a pine/aspen forest. Remote Sens. Environ. **112**: 2064–2073. doi:10.1016/j.rse.2007.08.023.

Dalponte, M., Bruzzone, L., and Gianelle, D. 2012. Tree species classification in the Southern Alps based on the fusion of very high geometrical resolution multispectral/hyperspectral images and LiDAR data. Remote Sens. Environ. **123**: 258–270. doi:10.1016/j.rse.2012.03.013.

Davies, A.B., and Asner, G.P. 2014. Advances in animal ecology from 3D-LiDAR ecosystem mapping. Trends Ecol. Evol. (Amsterdam), **29**(12): 681–691. doi:10.1016/j.tree.2014.10.005.

Erikson, M. 2004. Species classification of individually segmented tree crowns in high-resolution aerial images using radiometric and morphologic image measures. Remote Sens. Environ. **91**: 469–477. doi:10.1016/j.rse.2004.04.006.

Esseen, P.A., Ehnström, B., Ericson, L., and Sjöberg, K. 1997. Boreal forests. Ecol. Bull. **46**: 16–47. Available from https://www.jstor.org/stable/20113207.

Gauch, J.M. 1999. Image segmentation and analysis via multiscale gradient watershed hierarchies. IEEE Trans. Image Process. **8**(1): 69–79. doi:10.1109/83.736688.

Hardenbol, A.A., Kuzmin, A., Korhonen, L., Korpelainen, P., Kumpula, T., Maltamo, M., and Kouki, J. 2021. Detection of aspen in conifer-dominated boreal forests with seasonal multispectral drone image point clouds. Silva Fennica. **55**(4): article id 10515. 24. doi:10.14214/sf.10515.

Hovi, A., Raitio, P., and Rautiainen, M. 2017. A spectral analysis of 25 boreal tree species. Silva Fennica. **51**(4): article id 7753. 16. doi:10.14214/sf.7753.

Hyyppä, J., Kelle, O., Lehikoinen, M., and Inkinen, M. 2001. A segmentation-based method to retrieve stem volume estimates from 3-D tree height models produced by laser scanners. IEEE Trans. Geosci. Remote Sens. **39**(5): 969–975. doi:10.1109/36.921414.

International Union for Conservation of Nature. 2023. IUCN red list of threatened species. Available from https://www.iucn.org/resources/conservation-tool/iucn-red-list-threatened-species [assessed 20 October 2023].

Jonsell, M., Weslien, J., and Ehnstrom, B. 1998. Substrate requirements of red-listed saproxylic invertebrates in Sweden. Biodivers. Conserv. **7**(6): 749–764. doi:10.1023/A:1008888319031.

Kay, C.E. 1997. Is Aspen doomed? J. For. **95**(5): 4–11.

Kostensalo, J., Mehtätalo, L., Tuominen, S., Packalen, P., and Myllymäki, M. 2023. Recreating structurally realistic tree maps with airborne laser scanning and ground measurements. Remote Sens. Environ. **298**: 113782–. doi:10.1016/j.rse.2023.113782.

Kivinen, S., Koivisto, E., Keski-Saari, S., Poikolainen, L., Tanhuanpää, T., Kuzmin, A., et al. 2020. A keystone species, European aspen (*Populus tremula* L.), in boreal forests: ecological role, knowledge needs and mapping using remote sensing. For. Ecol. Manage. **462**: 118008–. doi:10.1016/j.foreco.2020.118008.

Korhonen, K.T., Ahola, A., Heikkinen, J., Henttonen, H.M., Hotanen, J.-P., Ihalainen, A., et al. 2021. Forests of Finland 2014–2018 and their development 1921–2018. Silva Fenn. **55**(5). doi:10.14214/sf.10662.

Korpela, I., Ørka, H.O., Maltamo, M., Tokola, T., and Hyyppä, J. 2010. Tree species classification using airborne LiDAR: effects of stand and tree parameters, downsizing of training set, intensity normalization, and sensor type. Silva Fenn. **44**(2): 319–339. doi:10.14214/sf.156.

Korpela, I., Polvivaara, A., Papunen, S., Jaakkola, L., Tienaho, N., Uotila, J., et al. 2023. Airborne dual-wavelength waveform LiDAR improves species classification accuracy of boreal broadleaved and coniferous trees. Silva Fenn. **56**(4):. doi:10.14214/sf.22007.

Kouki, J., Arnold, K., and Martikainen, P. 2004. Long-term persistence of aspen—a key host for many threatened species—is endangered in old-growth conservation areas in Finland. J. Nat. Conserv. **12**(1): 41–52. doi:10.1016/j.jnc.2003.08.002.

Kuuluvainen, T. 2002. Natural variability of forests as a reference for restoring and managing biological diversity in boreal Fennoscandia. Silva Fenn. **36**: 97–125. doi:10.14214/sf.552.

Kuzmin, A., Korhonen, L., Kivinen, S., Hurskainen, P., Korpelainen, P., Tanhuanpää, T., et al. 2021. Detection of European aspen (*Populus tremula* L.) based on an unmanned aerial vehicle approach in boreal forests. Remote Sens. **13**: 1723. doi:10.3390/rs13091723.

Latva-Karjanmaa, T., Penttilä, R., and Siitonen, J. 2007. demographic structure of European aspen (*Populus tremula*) populations in managed and old-growth boreal forests in eastern Finland. Can. J. For. Res. **37**(6): 1070–1081. doi:10.1139/X06-289.

Li, J., Hu, B., and Noland, T.L. 2013. Classification of tree species based on structural features derived from high density LiDAR data. Agric. For. Meteorol. **171-172**: 104–114. doi:10.1016/j.agrformet.2012.11.012.

Maltamo, M., and Packalen, P. 2014. Species-specific management inventory in Finland. *In* Forestry applications of airborne laser scanning. Dordrecht: Springer Netherlands. pp. 241–252. doi:10.1007/978-94-017-8663-8_12.

Maltamo, M., Næsset, E., and Vauhkonen, J. 2014. Forestry applications of airborne laser scanning: concepts and case studies.14th ed. Vol. 27. Springer Netherlands, Dordrecht. doi:10.1007/978-94-017-8663-8.

Maltamo, M., Pesonen, A., Korhonen, L., Kouki, J., Vehmas, M., and Eerikäinen, K. 2015. Inventory of aspen trees in spruce dominated stands in conservation area. For. Ecosyst. **2**: 12. Available from https://doi:10.1186/s40663-015-0037–4. doi:10.1186/s40663-015-0037-4.

Mikhail, E., Bethel, J., and McGlone, J., 2001. Introduction to modern photogrammetry. John Wiley & Sons, New York, pp. 479.

Myllymäki, M. 2016. On generalization of sample tree characteristics in the Finnish National Forest Inventory using linear mixed effects models. Natural Resources Institute Finland, Helsinki. p. 29.

Mäyrä, J., Keski-Saari, S., Kivinen, S., Tanhuanpää, T., Hurskainen, P., Kullberg, P., et al. 2021. Tree species classification from airborne hyperspectral and LiDAR data using 3D convolutional neural networks. Remote Sens. Environ. **256**: 112322–. doi:10.1016/j.rse.2021.112322.

Narendra, P.M., and Goldberg, M. 1980. Image segmentation with directed trees. IEEE Transactions on Pattern Analysis and Machine Intelligence, PAMI-2(2), 185–191. doi:10.1109/TPAMI.1980.4766999.

Næsset, E. 2002. Predicting forest stand characteristics with airborne scanning laser using a practical two-stage procedure and field data. Remote Sens. Environ. **80**(1): 88–99. doi:10.1016/S0034-4257(01)00290-5.

Næsset, E. 2014. Area-based inventory in Norway—from innovation to an operational reality. *In* Forestry applications of airborne laser scanning. Springer Netherlands, Dordrecht. pp. 215–240doi:10.1007/978-94-017-8663-8_11.

Näslund, M. 1937. Skogsförsöksanstaltens gallringsförsök i tallskog (Forest research intitute's thinning experiments in Scots pine forests). Meddelanden frstatens skogsförsöksanstalt Häfte 29 (In Swedish).

Ørka, H.O., Næsset, E., and Bollandsås, O.M. 2007. Utilizing airborne laser intensity for tree species classification. Int. Arch. Photogram. Remote Sens. Spat. Inform. Sci. **36**: W52.

Packalén, P., Suvanto, A., and Maltamo, M. 2009. A two stage method to estimate species-specific growing stock by combining ALS data and aerial photographs of known orientation parameters. Photogramm. Eng. Remote Sens. **75**(12): 1451–1460. doi:10.14358/PERS.75.12.1451.

Pippuri, I., Maltamo, M., Packalen, P., and Mäkitalo, J. 2013. Predicting species-specific basal areas in urban forests using airborne laser scanning data and existing stand register data. Eur. J. For. Res. **132**: 999–1012. doi:10.1007/s10342-013-0736-8.

R Core Team. 2022. R: a language and environment for statistical computing. R Foundation for Statistical Computing, Vienna, Austria. Available from https://www.R-project.org/.

Sasaki, Y. 2007. The truth of the F-measure. University of Manchester, MIB-School of Computer Science. Available from https://www.cs.odu.edu/~mukka/cs795sum11dm/Lecturenotes/Day3/F-measure-YS-26Oct07.pdf.

Säynäjoki, R., Packalén, P., Maltamo, M., Vehmas, M., and Eerikäinen, K. 2008. Detection of aspens using high resolution aerial laser scanning data and digital aerial images. Sensors (Basel, Switzerland), **8**(8): 5037–5054. doi:10.3390/s8085037.

Tikkanen, O.-P., Martikainen, P., Hyvärinen, E., Junninen, K., and Kouki, J. 2006. Red-listed boreal forest species of Finland: associations with forest structure, tree species, and decaying wood. Ann. Zool. Fenn. **43**(4): 373–383.

Toivonen, J., Kangas, A., Maltamo, M., Kukkonen, M., and Packalen, P. 2023. Assessing biodiversity using forest structure indicators based on airborne laser scanning data. For. Ecol. Manage. **546**: 121376–. doi:10.1016/j.foreco.2023.121376.

Torgo, L. 2016. SMOTE algorithm for unbalanced classification problems. R Package Version v1.1.0. Available from https://cran.r-project.org/web/packages/performanceEstimation/index.html [assessed 28 March 2023].

Tuominen, S., Näsi, R., Honkavaara, E., Balazs, A., Hakala, T., Viljanen, N., et al. 2018. Assessment of classifiers and remote sensing features of hyperspectral imagery and stereo-photogrammetric point clouds for recognition of tree species in a forest area of high species diversity. Remote Sens. **10**(5): 714–. doi:10.3390/rs10050714.

Vihervaara, P., Mononen, L., Auvinen, A., Virkkala, R., Lü, Y., Pippuri, I., et al. 2015. How to integrate remotely sensed data and biodiversity for ecosystem assessments at landscape scale. Landsc. Ecol. **30**(3): 501–516. doi:10.1007/s10980-014-0137-5.

Viinikka, A., Hurskainen, P., Keski-Saari, S., Kivinen, S., Tanhuanpää, T., Mäyrä, J., et al. 2020. Detecting European aspen (*Populus tremula* L.) in boreal forests using airborne hyperspectral and airborne laser scanning data. Remote Sens. **12**: 2610. doi:10.3390/rs12162610.

Wright, M.N., and Ziegler, A. 2017. Ranger: A fast implementation of random forests for high dimensional data in C++ and R. J. Stat. Softw. **77**(1): 1–17. doi:10.18637/jss.v077.i01.